From Visual Metrics to Public Perception: Mapping Nighttime Streetscapes in Nanjing's Old City, China

Xuan Zhu[1], Jiaying Shi[2], Wen You[3]

[1]Southeast University, Nanjing/China · xuanzhuseuarch@gmail.com
[2]Southeast University, Nanjing/China · shijiaying@seu.edu.cn (Corresponding author)
[3]Huazhong University of Science and Technology, Wuhan/China · M202470040@hust.edu.cn

Abstract: Nighttime streetscapes are critical to perceived safety and urban vitality, yet their perceptual quality remains difficult to quantify for planning and renewal. This study quantifies how image-derived visual metrics relate to public perception of nighttime streetscapes in Nanjing's Old City, China, and develops a street-level perception mapping framework. A total of 3,365 valid nighttime panoramic images were collected along the main road network. Fourteen objective visual metrics, covering brightness, color, and scene attributes, were computed for each image and mapped in GIS. Public perception of safety and aesthetics was assessed through a laboratory-based survey of selected images. Correlation analysis and stepwise regression were used to identify systematic relationships between visual metrics and perception. A Vision Transformer-based regression model was further trained to predict public perception of nighttime streetscapes. Together, these analyses demonstrate how interpretable visual metrics and data-driven modeling can be combined to quantify perceptual variation and support evidence-based diagnosis of nighttime street environments in historic urban areas.

Keywords: Nighttime streetscape, visual metrics, public perception, panorama, mapping

1 Introduction

Nighttime streetscapes shape perceptions of safety and comfort (FOTIOS et al. 2015) and influence whether people walk, stay, and engage with the city after dark (ZHU et al. 2023). Beyond roadway lighting, a growing body of nightscape research has examined how people evaluate nocturnal environments through affective impressions and experiential quality, including psychometric measurement tools such as the Nightscape Affect Index (GAO & ZHU 2025), evidence on fear-related responses under nighttime conditions (KIM et al. 2019), and studies showing that nighttime cityscape perceptions can differ from daytime readings in tourism and place evaluation contexts (HUANG & WANG 2018). In Nanjing's Old City, where historic street patterns and mixed everyday uses coexist, improving nighttime environments requires evidence that links visual experience to public perception, rather than relying on general claims of "better lighting" or "better design."

Existing research offers valuable insights but often separates measurable environmental properties from perception outcomes. Engineering-oriented studies emphasize physical quantities (WEI et al. 2025), while perception-oriented studies frequently rely on limited samples or less reproducible feature descriptions (KOO et al. 2022), making it difficult to compare results across streets and to support street-network diagnosis (FAN & BILJECKI 2024). Although nightscape studies increasingly connect subjective judgments with lighting and visual attributes – through protocols for sensorial perception and representation (ROBERT & FARHAT 2013), quantified links between subjective evaluation and objective lighting parameters (VALETTI et al. 2023), attention to chromatic appearance such as correlated color temperature (POURFATHOLLAH & MANDAVINEJAD 2020), and design-oriented evaluations of

Journal of Digital Landscape Architecture, 11-2026, pp. 886-898. © Wichmann Verlag, VDE VERLAG GMBH · Berlin · Offenbach. ISBN 978-3-87907-770-0, ISSN 2367-4253, e-ISSN 2511-624X, doi:10.14627/537770084.

visitor satisfaction in nightscapes – many remain case-specific and do not yield a comparable, segment-level diagnostic basis for everyday street networks. This gap is especially relevant for old-city contexts, where spatial variation is strong and planning decisions require segment-level prioritization.

To address this need, we combine panoramic street-view imaging, reproducible visual metrics, a structured perception survey, and modeling that supports both explanation and mapping. We extract fourteen metrics across brightness, color, and scene attributes, and measure perception using six indicators in two dimensions, safety and aesthetics. We then quantify associations using correlation analysis and stepwise regression, and extend perception estimation beyond the surveyed subset using a Vision Transformer-based regression model (Hou et al. 2024) with GIS visualization. By linking visual metrics to perception and producing spatial outputs at the street-network scale, the study offers a practical basis for evaluating and improving nighttime streetscapes in Nanjing's Old City.

2 Material and Methods

2.1 Data Collection

This study focuses on Nanjing's Old City and acquires nighttime streetscape samples through street-scale field imaging (Figure 1). To standardize shooting conditions as much as possible and to improve route execution efficiency, we adopted a one-direction capture strategy. Specifically, the street interface was continuously recorded along a predefined travel direction, avoiding back-and-forth shooting that could introduce variation in nighttime lighting conditions and duplicate samples.

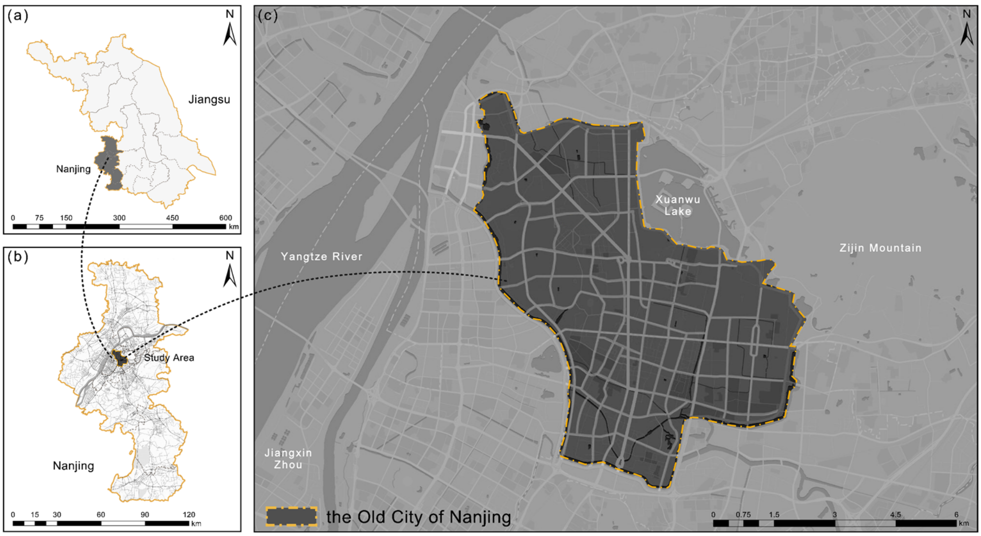

Fig. 1: Schematic diagram of research location

Panoramic street-view imagery was captured using an Insta360 X4 camera between December 15, 2024 and January 8, 2025, primarily from 19:00 to 21:00, when street lighting systems were fully operational. Images were collected at approximately 40 m intervals. Camera settings were fixed (ISO 6400, shutter speed 1/200 s, aperture f/1.9, auto white balance) to ensure consistent exposure and comparability across samples. In total, 3,378 nighttime panoramic images were obtained.

2.2 Objective Visual Metrics

To quantitatively characterize nighttime streetscapes, we constructed an indicator system consisting of 14 objective visual metrics derived from nighttime street-view images (Table 1). Following a light-color-scene framework, the metrics were grouped into brightness (n=4), color (n=5), and scene attributes (n=5), capturing illumination conditions, chromatic organization, and spatial composition.

Table 1: Objective visual metrics and semantic labels

<table>
<tr><th>Category</th><th>Metrics</th><th>Category</th><th>Metrics</th><th>Semantic Labels</th></tr>
<tr><td rowspan="10">1) Brightness Metrics</td><td rowspan="2">Mean Luminance</td><td rowspan="19">3) Scene Metrics</td><td rowspan="4">Spatial Enclosure, SE</td><td>Building</td></tr>
<tr><td>Wall</td></tr>
<tr><td rowspan="2">Luminance Contrast</td><td>Fence</td></tr>
<tr><td>Pole</td></tr>
<tr><td rowspan="3">High-luminance Spot Area Ratio, HSAR</td><td rowspan="2">Green View Index, GVI</td><td>Vegetation</td></tr>
<tr><td>Terrain</td></tr>
<tr><td>Sky View Factor, SVF</td><td>Sky</td></tr>
<tr><td rowspan="3">High-luminance Spot Count, HSC</td><td rowspan="4">Non-motorized View Index, NVI</td><td>Person</td></tr>
<tr><td>Sidewalk</td></tr>
<tr><td>Rider</td></tr>
<tr><td rowspan="9">2) Color Metrics</td><td rowspan="3">Mean CIELAB a*, Red-Green</td><td>Bicycle</td></tr>
<tr><td rowspan="8">Motorized View Index, MVI</td><td>Road</td></tr>
<tr><td>Traffic Light</td></tr>
<tr><td rowspan="3">Mean CIELAB b*, Yellow-Blue</td><td>Traffic Sign</td></tr>
<tr><td>Car</td></tr>
<tr><td>Truck</td></tr>
<tr><td>Mean Color Saturation, S</td><td>Bus</td></tr>
<tr><td>Color Complexity</td><td>Motorcycle</td></tr>
<tr><td>Color Harmony</td><td>Train</td></tr>
</table>

1) Brightness metrics describe overall luminance level, luminance variation, and localized high-intensity lighting, including Mean Luminance, Luminance Contrast, High-luminance Spot Area Ratio (HSAR), and High-luminance Spot Count (HSC).
2) Color metrics include Mean CIELAB a* (red-green), Mean CIELAB b* (yellow-blue), Mean Color Saturation, Color Complexity, and Color Harmony. While a*, b*, and saturation characterize overall chromatic tendency and intensity, Color Complexity and Color Harmony, derived from color composition and dominant-color organization (CHEN et al. 2025) – capture differences in visual richness and chromatic coordination.

3) Scene metrics are derived from semantic segmentation and aggregated into five composite features: Spatial Enclosure (SE), Green View Index (GVI), Sky View Factor (SVF), Non-motorized View Index (NVI), and Motorized View Index (MVI). These metrics represent interface enclosure, greenery visibility, openness, and the relative presence of traffic-related elements in nighttime street space.

2.3 Preprocessing and Extraction

To ensure geometric consistency across samples, all panoramic images were first standardized and cleaned (Figure 2). Because equirectangular projection introduces pixel-area distortion, images were converted to cylindrical equal-area projection using Mathematica (ZHANG et al. 2019). Low-quality samples (e. g., severe blur, exposure anomalies, occlusion, or missing metadata) were removed, resulting in 3,365 valid images.

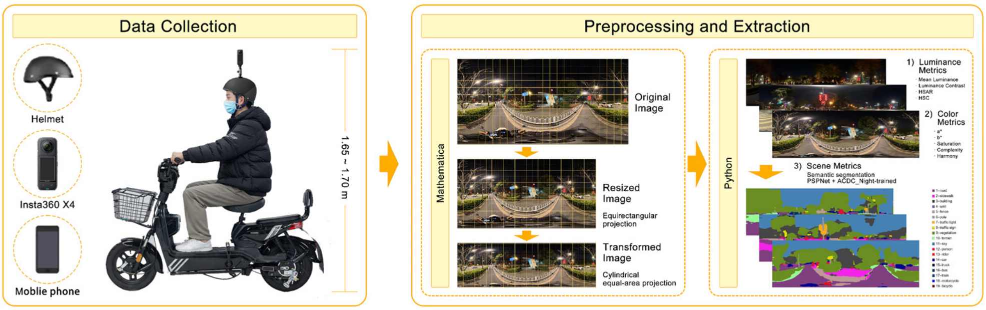

Fig. 2: Nighttime streetscape panorama data collection, preprocessing and extraction

The standardized images were then used to extract 14 objective visual metrics. Luminance metrics were derived using pixel-level statistics and threshold-based segmentation in Python. Color metrics were obtained by combining pixel-level statistics in CIELAB space with K-means clustering of dominant colors to derive Color Complexity and Color Harmony.

Scene metrics were extracted using deep-learning-based semantic segmentation. We applied PSPNet trained on the ACDC_Night dataset with Cityscapes-compatible labels to improve robustness under nighttime conditions (LIU et al. 2023). Class-wise pixel proportions were aggregated into five scene features (SE, GVI, SVF, NVI, and MVI), which served as quantitative inputs for subsequent analyses.

2.4 Perception Survey

To collect public perceptual evaluations of nighttime streetscapes, we conducted an image-based survey experiment. From the quality-controlled image set, 300 samples were selected at equal spatial intervals to ensure representativeness across the study area. The images were randomly assigned to 50 questionnaires, each containing a subset of samples. To improve rating stability, each image was evaluated five times by different participants, yielding multiple independent ratings per sample.

Perception was measured along two dimensions – Safety and Aesthetics – each represented by three indicators (Table 2). Safety included Lighting Safety (S1), Visual Openness (S2), and Traffic Safety (S3), while Aesthetics comprised Interface Diversity (A1), Color Pleasantness (A2), and Vegetation Richness (A3). Participants rated each image on all six items using a five-point Likert scale (1 = strongly disagree, 5 = strongly agree).

A total of 50 participants were recruited, including a professional student group (n = 25) and a general public group (n = 25), with balanced gender composition and an age range of 18–55 years. Individuals with visual, cognitive, or health conditions that could affect judgment were excluded. The resulting ratings provided the basis for reliability assessment, score aggregation, and subsequent modeling.

Table 2: Public perception indicators and codes

Dimensions	Perception Indicators	Indicator Codes
Safety	Lighting Safety	S_1
	Visual Openness	S_2
	Traffic Safety	S_3
Aesthetics	Interface Diversity	A_1
	Color Pleasantness	A_2
	Vegetation Richness	A_3

2.5 Analysis and Modeling

To ensure the stability and usability of survey ratings, inter-rater agreement and internal consistency were assessed. Intraclass correlation coefficients (ICC) were calculated for repeated ratings of the same image, and McDonald's ω and Cronbach's α were used to evaluate internal consistency within perception dimensions. When reliability was acceptable, ratings were averaged to obtain image-level scores; otherwise, robust aggregation or outlier removal was applied.

Prior to statistical modeling, objective metrics exhibiting strong skewness were transformed to improve distributional form, and all 14 metrics were standardized using Z-scores. Pearson correlation analysis was then conducted to examine (i) relationships among objective metrics, (ii) associations among perception indicators, and (iii) linkages between visual metrics and perception, with collinearity diagnostics used to screen redundant predictors.

Stepwise multiple linear regression was performed to model each of the six perception indicators separately, treating the 14 visual metrics as candidate predictors. Bidirectional selection was applied with entry and removal thresholds of $p < 0.05$ and $p > 0.10$, respectively. Final models were reported as regression equations, allowing comparison of key predictors and effect directions across indicators.

To complement explanatory regression with prediction-oriented modeling, we developed a Vision Transformer (ViT) regression model to capture potential nonlinearity and interaction effects. Survey-derived image-level scores served as supervision. To improve training stability with limited labels, images were augmented through projection conversion and horizontal mirroring, expanding the labeled dataset to 1,200 samples. The data were split into training and validation sets (80%/20%), and separate models were trained for each perception indicator. Predicted scores were then linked to image locations and visualized in GIS to reveal spatial disparities across the street network.

3 Results

3.1 Mapping of Objective Visual Metrics

Descriptive statistics for the 14 objective visual metrics are summarized in Table 3. Mean Luminance and Luminance Contrast show relatively concentrated distributions with clear central tendencies, indicating moderate variation in nighttime lighting across the study area. By contrast, HSAR and HSC are strongly right-skewed with upper outliers, suggesting that intense localized lighting is confined to a small subset of street segments.

Table 3: Descriptive statistics of the objective visual metrics

Objective Metrics	N	Median	Mean	Std. Deviation	Minimum	Maximum
Mean Luminance	3365	61.22	62.62	23.461	4.378	132.9
Luminance Contrast	3365	47.22	46.971	10.464	10.59	74.64
HSAR	3365	0.001	0.004	0.007	0	0.099
HSC	3365	15	21.696	19.798	0	162
Mean CIELAB a*	3365	2.43	2.663	1.815	-9.38	22.18
Mean CIELAB b*	3365	4.64	4.428	3.718	-21.08	21.73
Mean Color Saturation	3365	84.49	87.512	20.795	21.56	171.8
Color Complexity	3365	0.662	0.643	0.083	0.083	0.747
Color Harmony	3365	0.8	0.788	0.422	0.0005	2.126
SE	3365	27.716	28.329	10.031	3.018	64.65
GVI	3365	19.233	19.963	12.369	0	73.12
SVF	3365	8.38	10.288	8.751	0	41.87
NVI	3365	6.696	7.275	4.794	0	30.68
MVI	3365	33.291	34.145	7.893	8.677	89.66

Color metrics display substantial heterogeneity. Mean CIELAB a* and b* span both positive and negative values, indicating bidirectional shifts in chromatic tendency. Mean Color Saturation shows greater dispersion, reflecting variability in lighting color appearance across streets. Among dominant-color-derived metrics, Color Complexity exhibits relatively limited variation, whereas Color Harmony spans a wider range with more pronounced outliers, indicating that variation in chromatic coordination is more salient than differences in compositional richness.

Scene metrics also show marked heterogeneity. Several metrics approach zero for certain segments, indicating very low visibility of specific scene elements, while upper outliers suggest that strong enclosure, openness, greenery, or traffic presence is concentrated in a small number of streets.

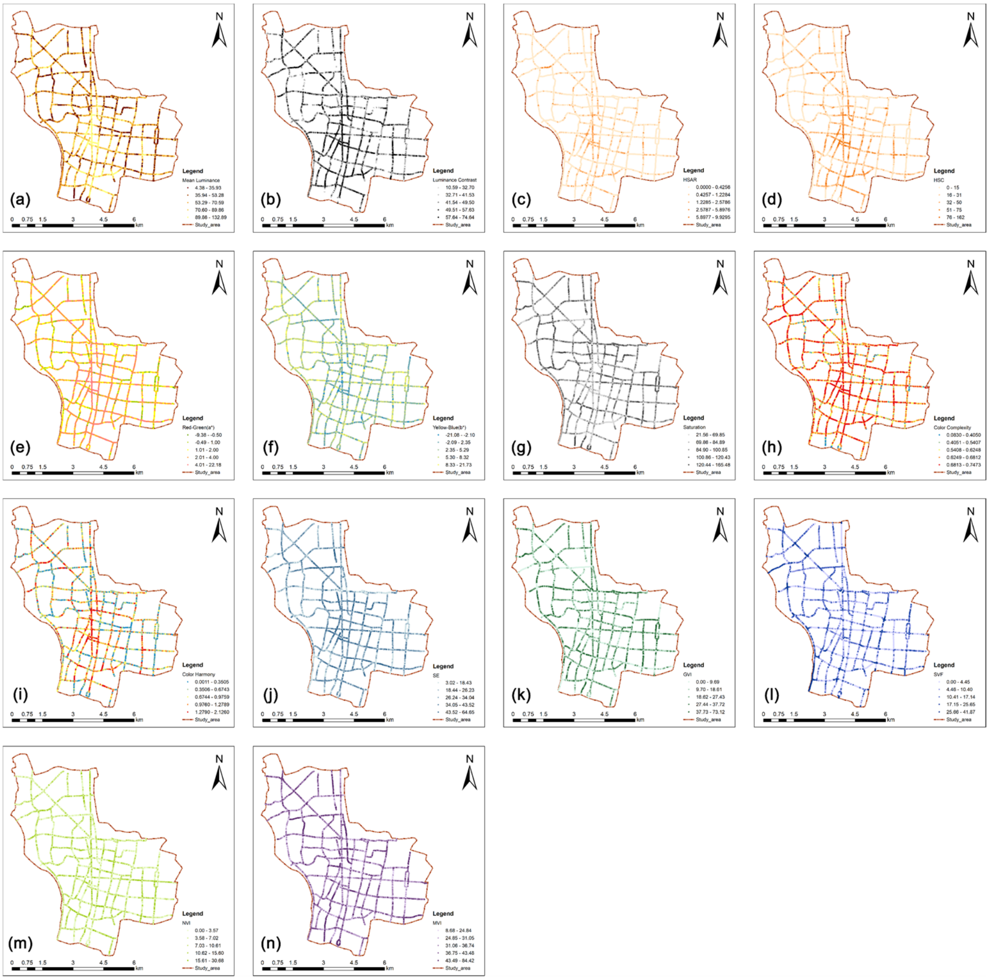

Fig. 3: Visualization of the 14 objective visual metrics:
(a) Mean Luminance, (b) Luminance Contrast, (c) HSAR, (d) HSC, (e) Mean CIELAB a*, (f) Mean CIELAB b*, (g) Mean Color Saturation, (h) Color Complexity, (i) Color Harmony, (j) SE, (k) GVI, (l) SVF, (m) NVI, (n) MVI

Spatial mapping reveals clear non-uniform patterns across all metrics (Figure 3). Luminance-related metrics are generally higher along major road corridors, whereas HSAR and HSC form localized hotspots at specific segments or nodes. Color metrics exhibit alternating linear and patchy patterns, and scene metrics reflect differences in street morphology and element composition. Overall, the metrics vary in complementary rather than uniform directions, providing an intuitive basis for identifying weaker street segments and proposing targeted nighttime improvement strategies.

3.2 Reliability of Public Perception

Survey reliability was assessed in terms of inter-rater agreement and internal consistency. Single-rating reliability (ICC(1,1)) ranged from 0.385 to 0.777, with higher values for Vegetation Richness (A3) and Lighting Safety (S1) and lower values for Color Pleasantness (A2). When five ratings were averaged for each image, ICC(1,5) increased substantially to 0.758–0.946, indicating high agreement across all indicators.

Internal consistency analysis yielded McDonald's ω = 0.759 (95% CI: 0.717–0.801) and Cronbach's α = 0.725 (95% CI: 0.677–0.772), both within acceptable ranges. These results support the use of five-rater mean scores as stable image-level perception measures for subsequent analyses.

3.3 Associations Between Visual Metrics and Perception

3.3.1 Correlation

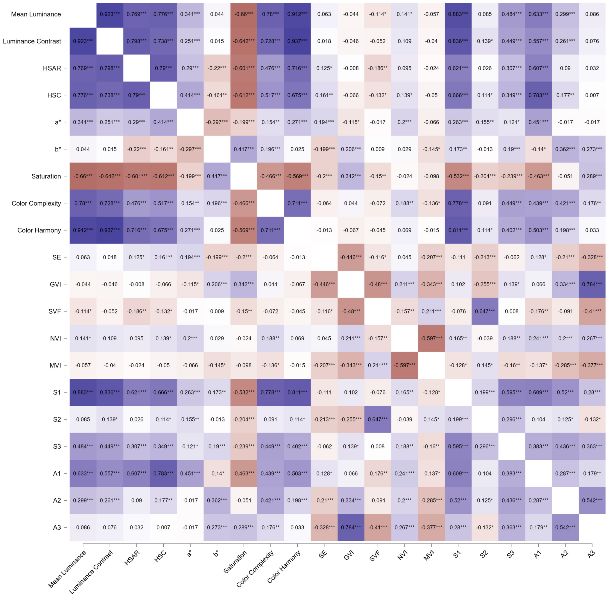

Fig. 4: Correlation matrix of objective visual metrics and subjective perception indicators (Pearson's r; * $p < 0.05$, ** $p < 0.01$, *** $p < 0.001$)

The correlation matrix between objective metrics and perception indicators is shown in Figure 4. Among objective metrics, luminance-related variables are strongly correlated, with Mean Luminance and Luminance Contrast exhibiting the highest association (r = 0.923). Both are positively related to HSAR and HSC, indicating that brighter scenes tend to display more localized high-luminance effects. Color Saturation is consistently negatively correlated with luminance-related metrics, suggesting a more desaturated appearance under stronger lighting conditions.

Scene metrics reveal structural trade-offs, including negative correlations between NVI and MVI (r = −0.597) and between GVI and SVF (r = −0.480). Within perception dimensions, indicators show stronger intra-dimension correlations than cross-dimension associations. Across dimensions, Lighting Safety is positively related to several aesthetic indicators, whereas Visual Openness exhibits weaker or negative associations with Vegetation Richness.

Associations between objective metrics and perception indicators are differentiated by perceptual dimension. Lighting Safety is most strongly related to luminance and color-organization metrics, Visual Openness is driven primarily by spatial structure, and Vegetation Richness is closely associated with GVI. These patterns motivate subsequent regression modeling and highlight the need to control multicollinearity among luminance variables.

Table 4: Stepwise regression results

Objective metrics	**Transform**	**S1**	**S2**	**S3**	**A1**	**A2**	**A3**
Mean Luminance	–	0.788	–	0.385	–	–	0.190
Luminance Contrast	–	–	–	–	–	–	–
High-luminance Spot Area Ratio	$\log_{10}(x+1)$	–	–	–	–	–	–
High-luminance Spot Count	$\log_{10}(x+0.0001)$	–	0.137	–	0.743	–	–
Mean CIELAB a*	–	–	0.099	–	0.152	–	–
Mean CIELAB b*	–	0.066	–	0.088	–	0.202	–
Mean color Saturation	$\log_{10}(x+1)$	–	–	–	–	-0.148	0.221
Color Complexity	x^3	0.144	–	–	–	0.239	0.102
Color Harmony	–	–	–	–	–	-0.107	–
Spatial Enclosure	$\log_{10}(x+1)$	-0.170	-0.159	–	–	–	–
Green View Index	$\log_{10}(x+1)$	–	–	0.167	0.116	0.186	0.753
Sky View Factor	$\log_{10}(x+1)$	–	0.517	0.132	–	–	–
Non-motorized View Index	$\log_{10}(x+1)$	–	–	–	0.089	–	–
Motorized View Index	$\log_{10}(x+1)$	-0.083	–	–	–	-0.076	-0.103
Intercept	–	3.740	3.613	3.313	2.954	3.252	3.342
Adjusted R^2	–	*0.830*	*0.496*	*0.291*	*0.652*	*0.352*	*0.657*
RMSE	–	*0.413*	*0.542*	*0.633*	*0.603*	*0.531*	*0.631*
N	–	300	300	300	300	300	300

Note. All variables undergo Z-score normalization after transformation before regression analysis.

3.3.2 Stepwise Regression

Stepwise regression selected key explanatory variables from the 14 objective nightscape metrics and established separate regression models for the six subjective perception indicators (Table 4). Because predictors were Z-score standardized after the necessary mathematical transformations, the coefficients reported in the table can be used to compare the relative direction and magnitude of different objective metrics' contributions to each perception indicator.

3.3.3 Machine Learning

In the explanatory stepwise regression models, fit varied substantially across indicators (RMSE = 0.413–0.633; Adjusted R^2 = 0.291–0.830). Indicators such as Traffic Safety (S3) and Color Pleasantness (A2) showed relatively limited linear fit, suggesting that visual-perception relationships may involve nonlinearity and interactions. In comparison, the ViT regression model achieved more favorable and more stable performance on an independent test set (RMSE = 0.382–0.551; R^2 = 0.436–0.853), outperforming stepwise regression overall (Table 5). We therefore used machine learning as a prediction-oriented pathway to extend limited survey labels into perception estimates with full coverage of the study area, supporting macro-level diagnosis and segment- and district-specific improvement strategies.

After linking the six predicted scores to sample locations, we produced road-network perception maps in ArcGIS. Safety-related indicators tended to form more continuous corridor-like gradients with localized high/low clusters, whereas Aesthetics-related indicators were more fragmented. Some segments showed synchronized variation in Interface Diversity, Color Pleasantness, and Vegetation Richness, while others did not.

Table 5: Machine-learning model performance on the validation set

Machine-Learning Models	N	MSE	RMSE	MAE	MAPE, %	R^2
Lighting Safety (S1)	240	0.153	0.391	0.276	8.815	0.853
Visual Openness (S2)	240	0.146	0.382	0.305	9.095	0.729
Traffic Safety (S3)	240	0.242	0.492	0.389	13.983	0.550
Interface Diversity (A1)	240	0.191	0.437	0.358	15.675	0.787
Color Pleasantness (A2)	240	0.280	0.529	0.443	15.893	0.436
Vegetation Richness (A3)	240	0.304	0.551	0.431	15.954	0.722

4 Discussion

The stepwise regression results indicate that different perception indicators align with different visual mechanisms. Lighting safety is most strongly associated with brightness conditions and with visual organization cues, suggesting that perceived safety depends on both overall visibility and how light is distributed in the scene. Visual openness is more sensitive to spatial-structure cues, particularly sky visibility and enclosure-related attributes, than brightness alone. This pattern is consistent with prior findings (Li et al. 2022). Vegetation richness is largely explained by green visibility (GVI) in our models, while aesthetic judgments also reflect how color and scene composition are organized (Song et al. 2025). The stepwise model reveals a negative effect of Color Harmony on color pleasantness, as it reflects a more uniform and potentially color monotonous appearance when saturation and complexity are controlled.

These findings support street-level implications for nighttime renewal in Nanjing's Old City. For safety-related experience, improving visual legibility can be as important as increasing illumination, highlighting the value of reducing extreme highlights, enhancing continuity along walking corridors, and coordinating chromatic appearance. For perceived openness, interventions that clarify sightlines and manage enclosure cues may be more effective than simply raising brightness. For aesthetic quality, vegetation visibility and controlled color composition emerge as key levers, informing planting strategies and heritage-sensitive lighting coordination at the segment scale.

Interpreting the GIS maps of predicted perception scores in relation to the four historic districts provides a planning-oriented reading of the model outputs (Figure 5). The district context helps clarify where perceived safety and aesthetic quality are relatively stronger or weaker across the old-city street network, offering an empirical basis for district-level prioritization in renewal and management.

Fig. 5: Spatial distribution of historic districts in Nanjing's old city and machine-learning predicted perception scores (S1–A3)
(a) Historic districts in Nanjing's Old City; (b) Lighting Safety, S1; (c) Visual Openness, S2; (d) Traffic Safety, S3; (e) Interface Diversity, A1; (f) Color Pleasantness, A2; (g) Vegetation Richness, A3

Distinct perceptual patterns emerge across the four historic districts. Chengnan exhibits a higher concentration of segments with favorable safety-related scores, particularly for lighting safety and visual openness, alongside stronger aesthetic ratings along key corridors, consistent with more continuous nighttime visibility and legible street scenes. In contrast, the Beijing East Road district contains several segments with relatively low traffic-safety scores, suggesting that motor-dominant corridors and complex intersections remain key perceptual constraints. The Gulou-Qingliangshan district shows comparatively strong vegetation-related aesthetics, reflecting hillside and park-adjacent settings that enhance nighttime green visibility. The Ming Palace district is more heterogeneous, with lower scores for interface diversity and vegetation richness along certain corridors, indicating constraints related to uniform frontages or reduced perceived greenery. Together, these contrasts imply differentiated renewal priorities across districts.

This district-based interpretation should be read as a planning-oriented synthesis rather than a strict zonal statistic. The maps visualize model-predicted scores derived from image-based inputs, and a more rigorous comparison across the four districts would require aggregating segment-level predictions within each district boundary and reporting means and uncertainty (WADOUX & HEUVELINK 2023). In addition, perception was measured through images rather than in-situ experience, and the data reflect a specific sampling period and one-direction capture strategy, which may not fully represent temporal variation or bidirectional pedestrian viewpoints across all streets (CURTIS et al. 2013).

5 Conclusion and Outlook

This study provides an end-to-end workflow to link visual metrics with public perception in nighttime streetscapes of Nanjing's Old City. Based on a large panoramic image dataset, fourteen objective metrics were extracted across brightness, color, and scene attributes, and six perception indicators were obtained from repeated public ratings with demonstrated reliability. Statistical analysis and stepwise regression quantified indicator-specific associations, and a Vision Transformer-based regression model produced network-wide perception predictions that were mapped in GIS. The workflow supports evidence-based diagnosis of spatial disparities in nighttime perception and helps prioritize street segments for renewal. Future research should incorporate multi-temporal sampling, on-site validation, and cross-city replication, and should further explore models that capture nonlinearity while retaining interpretability for planning and design practice.

References

CHEN, N., WANG, L., XU, T. & WANG, M. (2025), Perception of urban street visual color environment based on the CEP-KASS framework. Landscape and Urban Planning, 259, 105359. doi:10.1016/j.landurbplan.2025.105359.

CURTIS, J.W., CURTIS, A., MAPES, J., SZELL, A.B. & CINDERICH, A. (2013), Using Google Street View for systematic observation of the built environment: analysis of spatio-temporal instability of imagery dates. International Journal of Health Geographics, 12, 53. doi:10.1186/1476-072X-12-53.

FAN, Z. & BILJECKI, F. (2024), Nighttime Street View Imagery: A new perspective for sensing urban lighting landscape. Sustainable Cities and Society, 116, 105862. doi:10.1016/j.scs.2024.105862.

FOTIOS, S., UNWIN, J. & FARRALL, S. (2015), Road lighting and pedestrian reassurance after dark: A review. Lighting Research & Technology, 47 (4), 449-469. doi:10.1177/1477153514524587.

GAO, M. & ZHU, X. (2025), Development and testing of the nightscape affect index. Applied Psychology: Health and Well-Being, 17 (3), e70036. doi:10.1111/aphw.70036.

HOU, Y., QUINTANA, M., KHOMIAKOV, M., YAP, W., OUYANG, J., ITO, K., WANG, Z., ZHAO, T. & BILJECKI, F. (2024), Global Streetscapes – A comprehensive dataset of 10 million street-level images across 688 cities for urban science and analytics. ISPRS Journal of Photogrammetry and Remote Sensing, 215, 216-238.

HUANG, W.-J. & WANG, P. (2018), “All that's best of dark and bright”: Day and night perceptions of Hong Kong cityscape. Tourism Management, 66, 274-286. doi:10.1016/j.tourman.2017.12.006.

KIM, M., CHEON, S. & KANG, Y. (2019), Use of electroencephalography (EEG) for the analysis of emotional perception and fear to nightscapes. Sustainability, 11 (1), 233. doi:10.3390/su11010233.

KOO, B.W., GUHATHAKURTA, S. & BOTCHWEY, N. (2022), Development and validation of automated microscale walkability audit method. Health & Place, 73, 102733. doi:10.1016/j.healthplace.2021.102733.

LI, Y., YABUKI, N. & FUKUDA, T. (2022), Measuring visual walkability perception using panoramic street view images, virtual reality, and deep learning. Sustainable Cities and Society, 86, 104140. doi:10.1016/j.scs.2022.104140.

LIU, W., LI, W., ZHU, J., CUI, M., XIE, X. & ZHANG, L. (2023), Improving Nighttime Driving-Scene Segmentation via Dual Image-Adaptive Learnable Filters. IEEE Transactions on Circuits and Systems for Video Technology, 33, 5855-5867.

POURFATHOLLAH, M. & MAHDAVINEJAD, M. (2020), Viewerphilic nightscape based on correlated color temperature. Color Research & Application, 45 (1), 120-128. doi:10.1002/col.22450.

ROBERT, P. & FARHAT, G. (2013), Biophysical and cultural nightscapes: the three protocols for sensorial perception and representation of an artificial day. In: EAEA-11 Conference 2013, Track 2 “Experiential Simulation: the sensory perception of the built environment”, 273-280.

SONG, M. & XIAO, Y. (2025), Does Streetscape Color Matter for Urban Perceptions? A Deep Learning Approach to Street View Images. Land Use Policy, 155, 107581. doi:10.1016/j.landusepol.2025.107581.

VALETTI, L., PELLEREY, F. & PELLEGRINO, A. (2023), A Novel Approach for the Assessment of the Nocturnal Image of the Cultural Landscape. LEUKOS, 19 (1), 71-93.

WADOUX, A.M.J.-C. & HEUVELINK, G.B.M. (2023), Uncertainty of Spatial Averages and Totals of Natural Resource Maps. Methods in Ecology and Evolution, 14, 1320-1332. doi:10.1111/2041-210X.14106.

WEI, L., BIZJAK, G. & KOBAV, M. (2025), Evaluating the impact of road lighting on pedestrian reassurance through the day-dark approach. Lighting Research & Technology, 57, 264-277. doi:10.1177/14771535241269699.

ZHANG, W., ZHOU, Y. X., & YANG, M. Q. (2019), Research on Automatic Identification and Measurement of Panoramic Visible Green Index. Landscape Architecture, 26 (10), 89-94. doi:10.14085/j.fjyl.2019.10.0089.06.

ZHU, M., TENG, R., WANG, C., WANG, Y., HE, J. & YU, F. (2023), Key Environmental Factors Affecting Perceptions of Security of Night-Time Walking in Neighbourhood Streets: A Discussion Based on Fear Heat Maps. Journal of Transport & Health, 32, 101636.